UAB
Universitat Autònoma de Barcelona

Dipòsit digital de documents de la UAB

This is the **accepted version** of the journal article:

Limage, Rhodesherdeline [et al.]. «TiO2 Nanoparticles and Commensal Bacteria Alter Mucus Layer Thickness and Composition in a Gastrointestinal Tract Model». *Small (Weinheim)*, Vol. 16, Num. 21 (May 2020), art. 2000601 DOI 10.1002/smll.202000601

This version is available at https://ddd.uab.cat/record/325659

under the terms of the IN COPYRIGHT license.

TiO_2 Nanoparticles and Commensal Bacteria Alter Mucus Layer Thickness and Composition in a Gastrointestinal Tract Model

Rhodesherdeline Limage[1], Elad Tako[2], Nikolai Kolba[2], Zhongyuan Guo[1], Alba García-Rodríguez[1,4], Cláudia N. H. Marques[3,4], and Gretchen J. Mahler[1,4*]
[1]Department of Biomedical Engineering, Binghamton University, Binghamton, NY, USA
[2]USDA-ARS, Robert W. Holley Center for Agriculture and Health, Ithaca, NY, USA
[3]Department of Biological Sciences, Binghamton University, Binghamton, NY, USA
[4]Binghamton Biofilm Research Center, Binghamton University, Binghamton, NY, USA

*Correspondence to Gretchen Mahler, PhD, Binghamton University, Department of Biomedical Engineering, PO Box 6000, Binghamton, NY 13902
Phone: 607-777-5238
Fax: 607-777-5780
E-mail: gmahler@binghamton.edu

Keywords: titanium dioxide, microbiota, ingestion, *in vitro* digestion

Abstract:

Nanoparticles (NPs) are used in food packaging and processing and have become an integral part of many commonly ingested products. There are few studies that have focused on the interaction between ingested NPs, gut function, the mucus layer, and the gut microbiota. In this work, an *in vitro* model of gastrointestinal (GI) tract was used to determine whether, and how, the mucus layer is affected by the presence of Gram-positive, commensal *Lactobacillus rhamnosus*; Gram-negative, opportunistic *Escherichia coli*; and/or exposure to physiologically relevant doses of pristine or digested TiO_2 NPs. Caco-2/HT29-MTX-E12 cell monolayers were exposed to physiological concentrations of bacteria (expressing fluorescent proteins) and/or TiO_2 nanoparticles for a period of 4 hours. To determine mucus thickness and composition, cell monolayers were stained with alcian blue, periodic acid schiff, or an Alexa Fluor® 488 conjugate of wheat germ agglutinin. It was found that the presence of both bacteria and nanoparticles alter the thickness and composition of the mucus layer. Changes in the distribution or pattern of mucins can be indicative of pathological conditions, and this model provides a platform for understanding how bacteria and/or NPs may interact with and alter the mucus layer.

Introduction

Nanoparticles (NPs), deriving from the Greek word "nano" meaning extremely small, are defined as clusters of atoms ranging from 1-100 nanometers that serve numerous purposes in consumer products. Many types of food contain nanoparticles, whether they are organic, inorganic, intentionally or unintentionally added during the manufacturing process. Nanoparticles, specifically metal oxide nanoparticles, are often added to food to improve or enhance food texture, flavor, and/or nutrient stability.[2] As nanomaterials are incorporated in storage containers and food packaging, NP-food cross contamination is expected.[3] Human ingestion of nanoparticles through food, food packaging, and other consumer products is therefore nearly unavoidable.[4] Titanium dioxide (TiO_2) NPs are widely used in consumer food products due to whitening pigment and opacifying characteristics.[5,6] The highest concentration of TiO_2 NP fractions are found in the coating constituent of sweets, candies, and chewing-gums.[5,7] Previous studies have estimated that daily exposure to TiO_2 NPs via ingestion ranges between 1-2 mg TiO_2/kg b.w. in US children under 10 years of age, and 0.2-0.7 mg TiO_2/kg b.w. in US adults.[5,8,9] However, these estimations have been refined recently and the range of exposure was reported to be between 5.5-10.4 mg/kg b.w. in children depending on the exposure scenario.[9] Referred to as food grade nanoparticle in Europe, E171 can contain approximately 43% of TiO_2 NPs, and has been found to be absorbed in the GI tract at low levels.[7,9,10]

Models of the gastrointestinal (GI) tract have been used as a means to understand the potential toxic or functional effects of exposure to NPs as a food additive.[2,6,7,11] The small size of NPs allows them to cross cellular barriers and can lead to free radical formation in tissues and oxidative damage to the cells that line the GI tract or the mucus layer.[12,13] The GI tract, particularly the small intestine, plays a major role in ingestion, digestion and absorption of nutrients, and the elimination of non-digested foods and microbial products[2,14–16]. The mucosal surface of the GI tract is a complex environment of epithelial cells, immune cells and is colonized by microbiota.[17] Covered by mucin-secreting goblet cells and other substances that make up the GI mucus layer, the intestinal epithelium serves as the first line of defense against attachment and invasion of microorganisms, including commensals and pathogens.[14,17,18] Commensal bacteria normally fail to reach intestinal epithelial cells since they are trapped in the mucus layer and often discarded through peristaltic movement.[14] The major goblet cell mucins in the small and large intestine are MUC2 proteins, which are gel-forming secretory mucins localized in clusters.[19–21] Goblet cells synthesize and secrete bioactive molecules such as secretory and membrane associated mucins, trefoil peptides, resistin-like molecule beta (RELMβ), and Fc-γ binding protein (Fcgbp); Paneth cells secrete antimicrobial peptides (beta defensin and lysozymes); and enterocytes secrete secretory IgA; which are all components of mucus.[14] Epithelial mucins are further classified into neutral and acidic grouped sialo- and sulphomucins depending on the sialic acid or ester sulphate radicals with hexosamine.[22] Neutral mucins are neutral glycoproteins with immunologically-active carbohydrate and protein containing substances, whereas acidic mucins are composed of sulfo/sialomucins.[22–24] Few studies have been performed on the intestinal mucus lining with the intent to better understand the role it plays as a protective barrier, and to determine how it is affected by bacteria present in the gut or by ingested food additives.[20,25,26]

The interaction between the human intestine and its microbiota is mediated by an intervening mucus layer that is secreted by the intestinal epithelial cells along the apical surface.[27] Similar to the gut microbiota, mucus thickness also varies throughout the length of the intestine. Studies have identified that the GI mucus forms a single, easily removable layer in the small intestine and a double layer firmly attached to the colon epithelium.[21,28,29] These mucus layers are organized around the MUC2 mucin to form a large, net-like polymer that is permeable to gases, water and nutrients, but impermeable to most microorganisms.[20] Mucus lubricates the GI epithelium to facilitate protection from excessive mechanical stress by dietary components, corrosive action of gastric acid, and from proteolysis by

digestive enzymes.[30] It also prevents infection by binding bacteria or viruses through specific interactions with carbohydrate chains. Despite being smaller than the average mucus mesh pore size, the majority of particles administered orally are not able to be transported through the GI mucus and/or they are likely to be trapped by mucus via adhesive forces (hydrophobic interactions) or are rapidly eliminated.[31,32] It has previously been found that Norwalk (38 nm) and human papilloma virus (HPV; 55 nm) are able to penetrate the mucus layers at a rate identical to water.[32] Additionally, it has been demonstrated that TiO_2 NPs were able to permeate the mucus layer into the underlying tissue, regardless of their size and hydrophilicity/hydrophobicity.[20] A number of *in vivo* studies further suggest that nanoparticles are able to enter the epithelium through M-cells, since no mucus is secreted in the region surrounding these cells and particulate uptake by the mammalian GI tract mainly occurs via Peyer's patches.[33] These previous findings strongly establish that NPs are able to diffuse through low viscosity pores in the mucin fiber matrix, assuming they do not adhere to the mucus, because small molecules are unable to form polyvalent adhesive bonds with the mucus gel.[31–33]

The human GI tract contains trillions of microorganisms, including bacteria, viruses and fungi.[34,35] These microorganisms form the intestinal microbiota, which plays a crucial role in GI tract physiologic functions such as gastric secretion, gut motility, mucosal permeability and barrier function, visceral sensitivity and mucosal blood flow. [36,37] The gut microbiota aids in food digestion, and plays a critical role in the absorption of nutrients from some indigestible foods.[38] Additionally, bacteria present in the gut microbiota inhabit exposed mucosal surfaces and have been shown to inhibit pathogenic bacteria colonization by producing antimicrobial compounds, which also protect the intestinal epithelium from the harmful effects of pathogens.[34,39] However, epithelial invasion by pathogens or certain commensal bacteria can occur and disturb the barrier's function, thus increase gut permeability.[35] This primarily occurs following bacterial production of specific mucin-degrading enzymes that release monosaccharides attached to the mucin glycoproteins.[19] Previous studies have shown that commensal bacteria such as *Lactobacillus* sp. were likely to increase the production of MUC2 and MUC3 mucins and hinder the attachment of enteropathogenic *Escherichia coli*, indicating that enhanced mucus layers together with the presence of *Lactobacillus* sp. provides protection against invasion by pathogens.[14,18] One example is *L. rhamnosus GG*, a Gram-positive bacterium that behaves as a probiotic to promote better health, leading to an increase in the production of mucins to stimulate intestinal epithelial cell barrier response.[34]

Due to the symbiotic relationship between bacteria and the human intestinal cells, it is important to assess the impact of NPs on the gut microbiota. Commensal bacteria have a major impact on immunophysiological functions by inducing protective responses that prevent colonization and invasion of pathogens.[40] Previous *in vitro* studies, performed to provide insights into mechanisms that may be overshadowed by *in vivo* systems, have shown that toxicity effects in both Gram-positive and Gram-negative bacterial species can be dependent of the photocatalytic activity of TiO_2 NPs.[41] The photocatalytic-mediated toxicity of TiO_2 NPs can also inhibit the growth of commensal bacteria in an *in vitro* insect model in the absence of light, but not *in vivo*.[39] *In vitro* microbiome models and *in vivo* studies have shown that exposure to food-grade TiO_2 NPs (E171, 25 nm) can induce compositional shifts in microbiota. Although the shift in abundance of bacterial species did not display measurable physiological changes in the GI tract in one study, a separate study demonstrated that TiO_2 did promote biofilm formation of commensal bacteria, resulting in an alteration in the release of bacterial metabolites of mucin gene expression by the gut epithelial cells.[42,43] In addition, it has also been found that silver NPs have the potential to disrupt the intestinal microbiome.[20] Minimal and non-statistically significant changes in GI microbiota following exposure to TiO_2 have also been observed in mice.[41] Studies have reported that exposing *E. coli* to TiO_2 NPs resulted in an induction of oxidative stress, of changes on the bacterial wall morphology, and changes in the membrane permeability and osmotic balance

regulation.[44] While it is unclear what factors led to these *in vivo-in vitro* discrepancies, these studies highlight how the presence of ingested nanoparticles can amplify or negate changes in the microbiota.

The primary objective of this study is to understand how exposure to TiO_2 NPs at physiologically relevant doses and the presence of Gram-positive *L. rhamnosus* (beneficial) or the Gram-negative *E. coli* (opportunistic) affect the production and composition of the intestinal mucus layer. Throughout the GI tract there are mucus cells filled by both neutral and non-sulfated acidic mucins. Changes in the distribution or pattern of acidic and neutral mucins are involved in inflammation and cancer.[45,46] While enterocyte-like (Caco-2) intestinal epithelial cells possess membrane-bound mucins, they do not produce secreted mucins such as MUC2 and MUC5AC, the main secreted gel forming mucins in the GI tract[47]. Therefore an *in vitro* model of the GI tract with co-cultures of Caco-2 and mucus-producing cells (HT29-MTX-E12), representing the mucus-secreting goblet cells of the intestine, were utilized to evaluate properties of the mucus following exposure to TiO_2 NPs, bacteria or both. This model provides a platform for understanding changes in the mucus layer, understanding disease pathogenesis, and/or studying therapeutic options such as the manipulation of the gut microbiota to address and diagnose chronic inflammatory gut diseases.

2. Results

2.1. NP characteristics and behavior in dispersants

The nanoparticles used in this study (30 nm anatase TiO_2 nanoparticles, US3498US, Research Nanomaterials, Inc, Houston, TX) were previously characterized.[8] Transmission electron microscopy analysis showed that TiO_2 NPs sizes were within manufacturer's range (**Table 1**).[8,48] Briefly, primary sizes of TiO_2 were demonstrated to range between 20-40 nm, which was found to be consistent with manufacturer-reported values. The behavior of TiO_2 NPs in suspension was assessed through dynamic light scattering (DLS) using a Zetasizer Nano ZS90 (Malvern Panalytical Ltd.). TiO_2 NPs ranged from 332 ± 42 nm in water and 355 ± 70 nm in serum free DMEM which suggested the formation of aggregates in solution.[8,48] A tendency toward agglomeration was shown with the size of agglomerates increasing based on dispersant (polydispersity index: 0.34-0.49 in 18 MΩ water and 0.42-0.54 in DMEM).[8] The hydrodynamic diameter of digested TiO_2 NPs was 220.9 ± 44.8 nm in digested dispersants (**Table 1**). The polydispersity index (PdI) of digested TiO_2 NPs, generated by the Malvern software, was 0.509 ± 0.073. The digested TiO_2 NPs had a ζ potential of -13.0±1.8 mV (**Table 1**). In contrast, simulated gastrointestinal tract fluid reduced the hydrodynamic sizes of TiO_2 NPs when compared with culture medium. Porcine pepsin and pancreatin/bile enzymes in the digestion solution may affect the detection and measurement of NPs properties at any NP concentration. The simulated gastrointestinal tract fluid increased the ζ potentials of digested TiO_2 NPs when compared with undigested NP in culture medium. The digested TiO_2 NPs have large, negative ζ-potentials, meaning that they strongly repel each other to prevent aggregation. A high ζ-potential, especially more negative than -30mV reflects the stability of the dispersant system.[49] The sizes measured by DLS were larger than the primary particle diameters shown in TEM images because the NP agglomerates when suspended in water.[8]

Table 1. Characterization of digested and undigested TiO_2 nanoparticles

Concentration	µg/mL	0.14
	Particle/mL	2.3 x 10^9
Undigested NP in Serum Free DMEM [8]	$d_{h,z\text{-average}}$ (nm)	874±93
	PdI	0.611±0.042
	ζ (mV)	-23.4±0.5
Digested NP	$d_{h,z\text{-average}}$ (nm)	221±45
	PdI	0.509±0.073
	ζ (mV)	-13±1.8

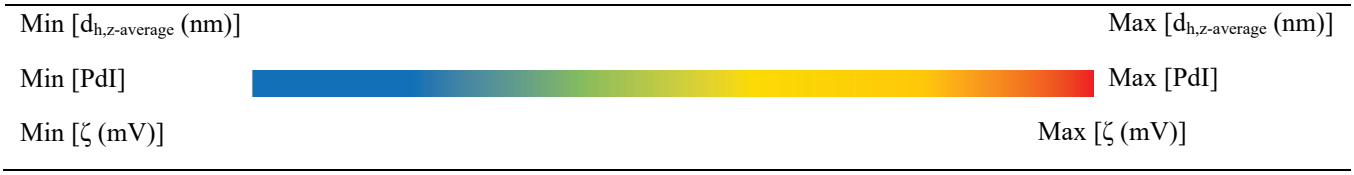

2.2. Evaluation of mucus production/staining assays

Co-cultures of Caco-2/HT29-MTX-E12 grown in either a 24-well plate, coverslips within a 6-well plate or on a polycarbonate membrane for 2 weeks at a ratio of 3:1, to represent small intestinal epithelium, developed a visible and continuous mucus layer. Secreted mucus along the barrier formed by the monolayer was evaluated using alcian blue (AB) and periodic acid-Schiff (PAS) staining. AB is a histochemical dye that stains glyco-polysaccharide and muco-polysaccharide or acidic mucosubstances. AB staining indicated that acidic mucins are spread throughout the cell monolayer to serve as a protective barrier prior to and after exposure to TiO_2 NPs. Monoculture of Caco-2 cells do not produce mucus and showed only background levels of staining when compared to staining of Caco-2/HT29-MTX-E12 conditions (**Figure 1A**). Monocultures of HT29-MTX-E12 and co-culture of Caco-2/HT29-MTX-E12 showed more intense staining when exposed to TiO_2 compared to that of unexposed cells (**Figure 1B, C**). To quantitatively assess the amount of acidic mucosubstance, the amount of blue color generated from the dye was measured and it was shown that there was an increase in intensity following exposure to pristine TiO_2 NPs alone and pristine TiO_2 NPs combined with bacteria (**Figure 1D, F**). An increase in intensity was also observed following exposure to digest and *L. rhamnosus* with digest compared to negative controls with DMEM only (**Figure 1G**). An increase in intensity was observed following co-exposure to pristine TiO_2 NPs and *E. coli* (**Figure 1D**). However, no significant changes were observed following co-exposure to digested TiO_2 NPs and *E. coli* (**Figure 1E**).

[insert **Figure 1**]

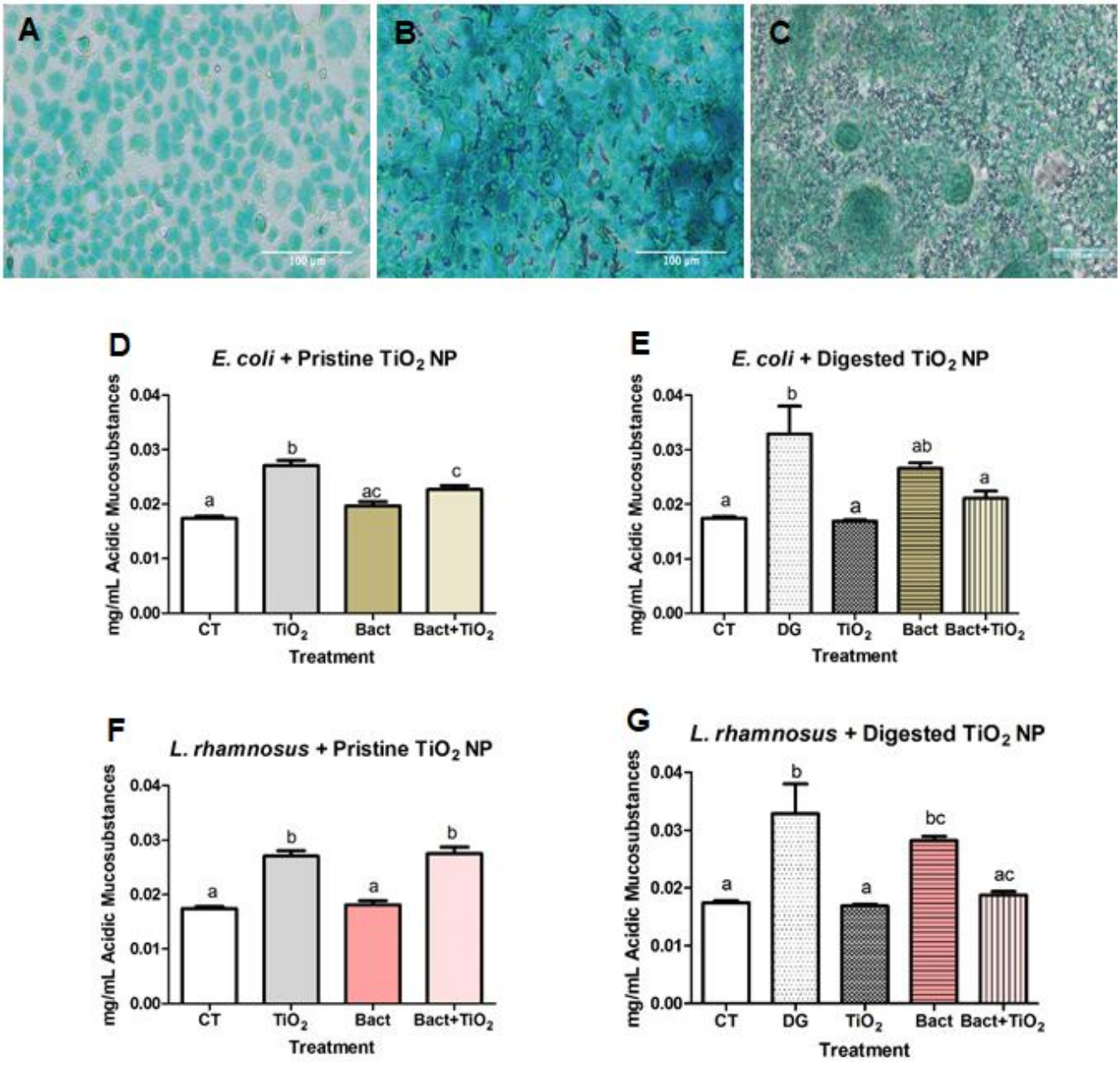

Neutral and sialic acid containing mucosubstances were then quantified using PAS, and higher levels of neutral and/or sialic acid containing mucosubstances were detected in Caco-2/HT29-MTX-E12 exposed to TiO_2 NPs, both pristine and digested. PAS results showed that neutral and/or sialic acid containing mucosubstances secretions significantly increased in the presence of bacteria (with or without digest), stomach digest, pristine TiO_2 NPs and following co-exposure to non-digested TiO_2 NPs and *L. rhamnosus* (**Figure 2A, B, C, D**). However, there was a significant decrease following co-exposures to digested TiO_2 NP and *E. coli* (**Figure 2B**).
[insert **Figure 2**]

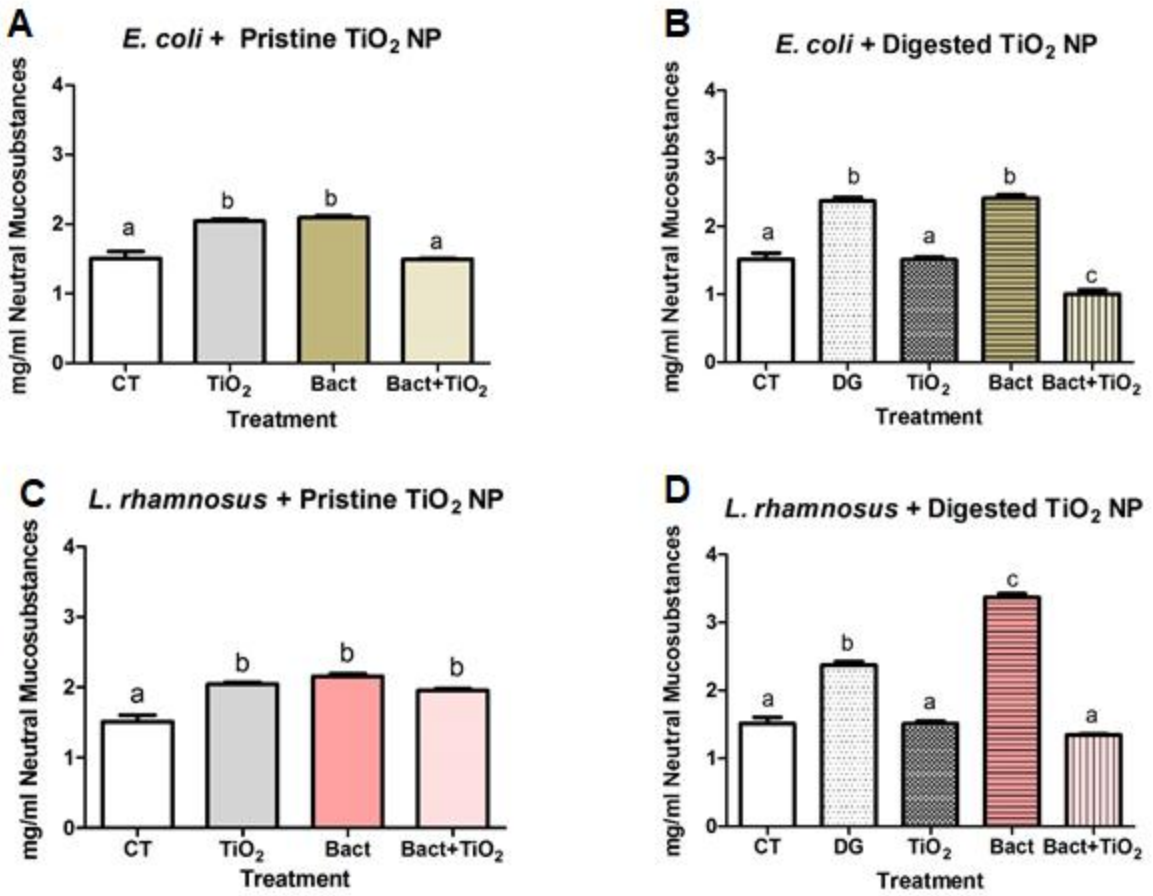

2.3. Histochemical analysis of mucus secretion

The combination of alcian blue and PAS was used to differentiate acidic mucins from neutral mucins present in the monolayer of Caco-2/HT29-MTX-E12. Sections were cut and stained with standard alcian blue, pH 2.5 followed by PAS. Acidic mucins were stained deep blue while neutral mucins had a bright magenta color. When both type of mucins were present, the color was a dark purple which can be seen in the displayed image of the monolayer of mucus producing HT29-MTX-E12 (**Figure 3A**). Co-cultures of Caco-2/HT29-MTX-E12 were also stained following different exposure conditions using both staining methods and the average of overall mucus layer thickness was quantified (**Figure 3B, C and Table 2**). The mucus thickness increased following both exposure to bacteria and co-exposure to both *E. coli* or *L. rhamnosus* and TiO_2 compared to unexposed cells. However, co-exposure to *L. rhamnosus* and TiO_2 NPs reinstated a decreased mucus thickness, albeit still increased compared to controls. In contrast, co-exposure to *E. coli* and TiO_2 NPs further increased the mucus thickness, indicating that the interaction of TiO_2 NPs with the bacteria varies.

[insert **Figure 3** and **Table 2**]

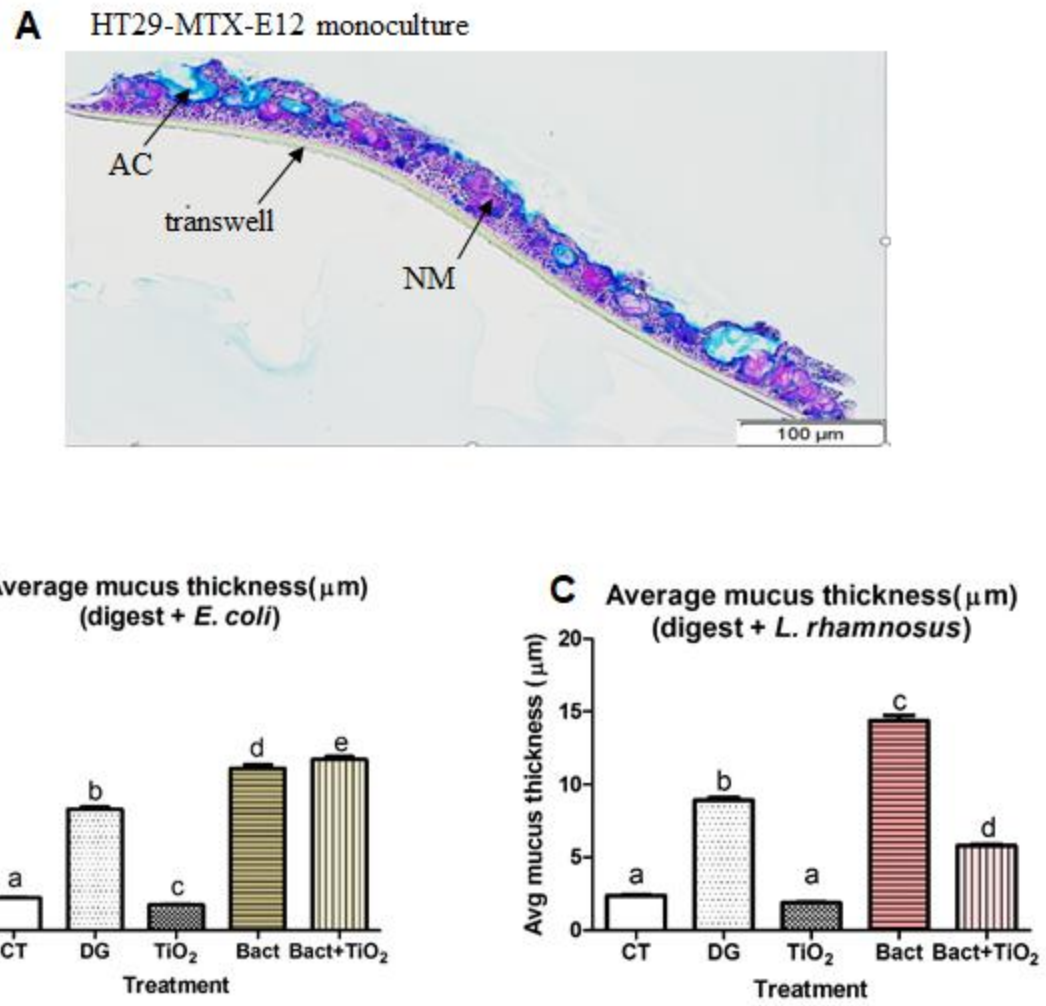

Table 2. Average mucus thickness following NP and bacteria exposure

Treatment	**Avg Mucus thickness (µm)**	**SEM**
Control (DMEM only)	2.388	0.052
E. coli	4.008	0.134
L. rhamnosus	3.226	0.125
Digest	8.93	0.176
Digested TiO_2	1.884	0.048
Digested *L. rhamnosus*	14.38	0.357
Digested *E. coli*	11.95	0.258
Digested TiO_2 & *L. rhamnosus*	5.810	0.084
Digested TiO_2 & *E. coli*	12.61	0.208

2.4. Visualization/quantification of mucus by Confocal Laser Scanning Microscopy

To further visualize and quantify the mucus layer of the intestinal epithelial barrier, the samples were analyzed using confocal microscopy. Bacteria were transformed with mCherry to express red fluorescence. With the use of different fluorochromes at particular excitations, the distinction between various barrier structures including the mucus layer was made possible. Hoechst and WGA were used to stain the nucleus and the mucins secreted respectively (**Figure 4**). The various components of the *in vitro* model with mucus layer were present on the monolayer surface while entrapped bacteria were present within the monolayer. Z-scans of a wide area of the monolayer were performed and many transversal cuts were obtained to better distinguish the mucus layer and bacteria interactions from the other components of the cells (**Figure 5**). The images obtained from the scan confirm the interaction observed in the quantifying methods of AB/PAS, specifically that an increase in the mucus layer was observed in the presence of bacteria alone and bacteria combined with digested TiO_2 NPs when compared to unexposed cells. However, exposure to TiO_2 NPs alone did not result in a drastic change in the mucus layer.

[insert **Figure 4**]

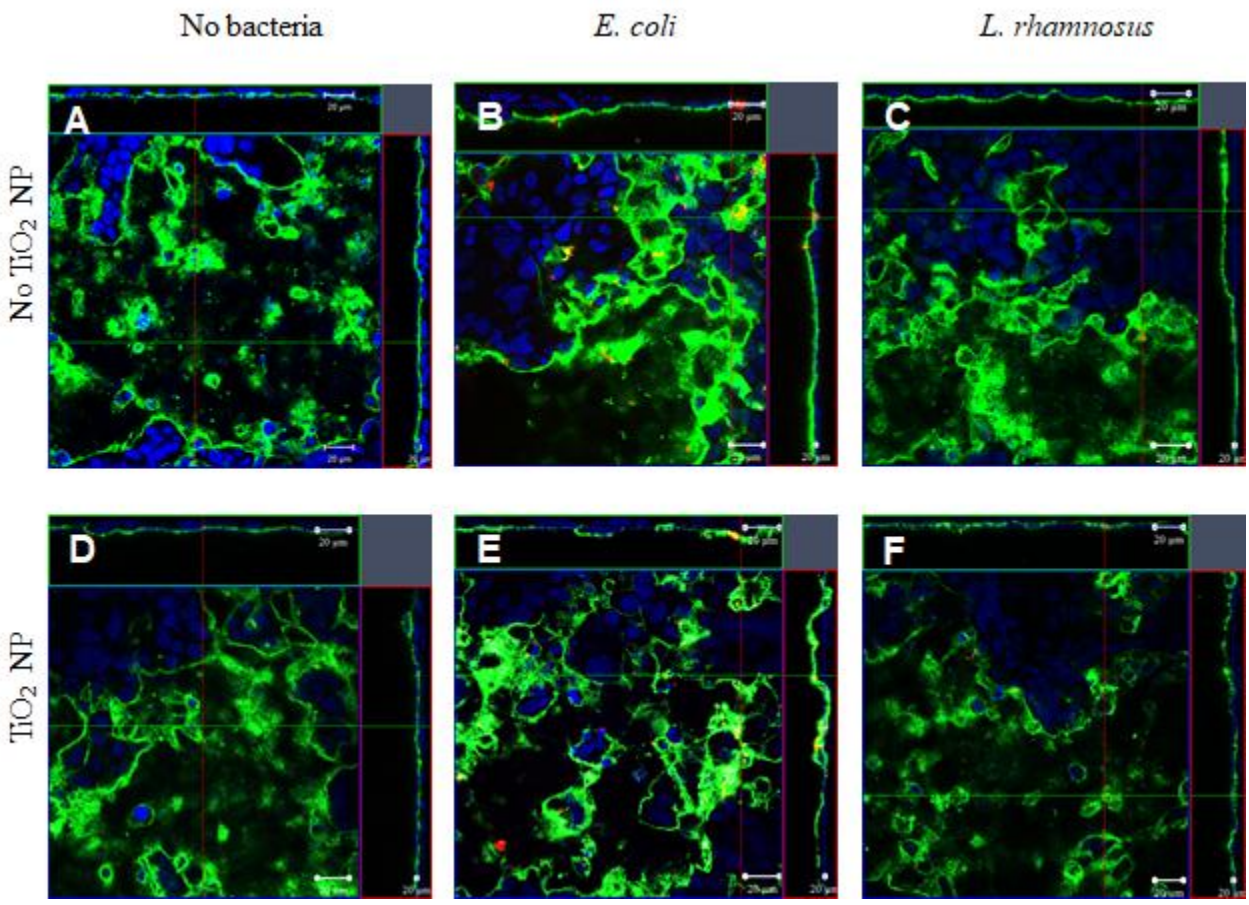

[insert **Figure 5**]

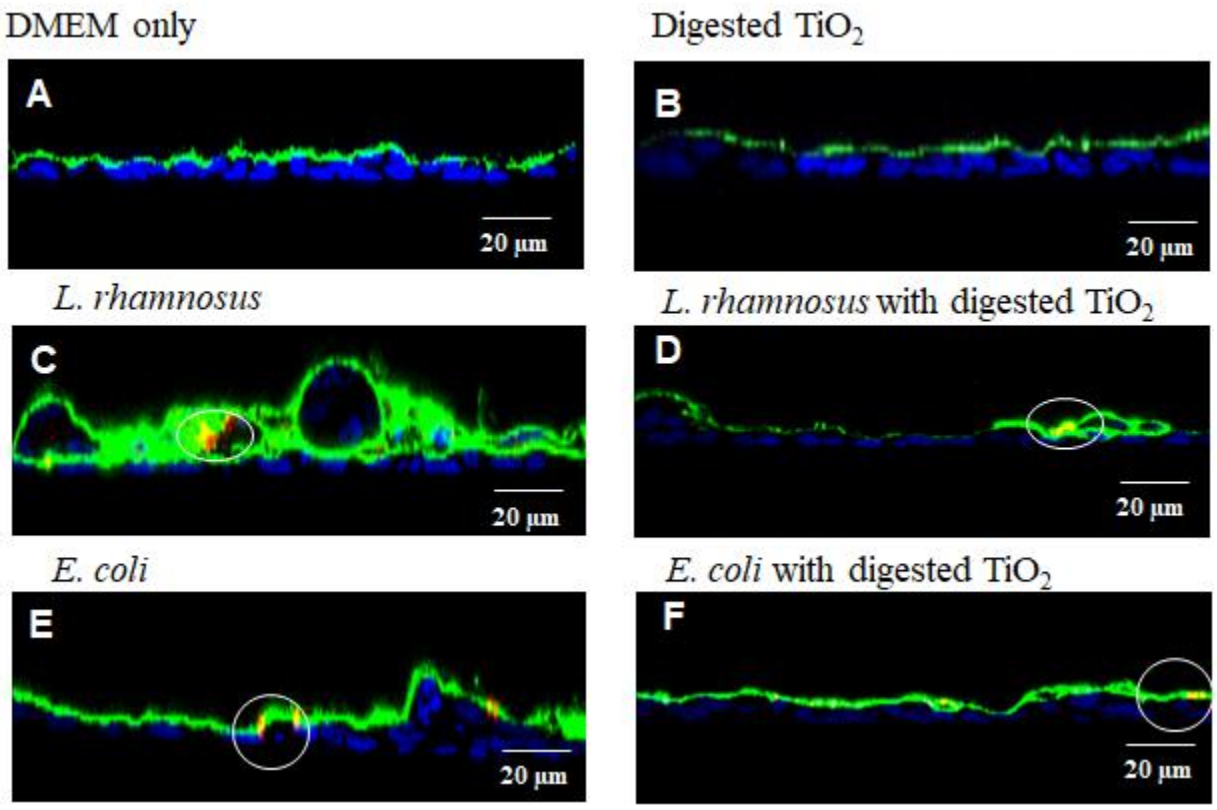

3. Discussion

While the production and the use of nanomaterials or nanosized particles as food additives are growing, information on their potential effects on human health, particularly the mucus layer lining the GI tract, are still lacking. This is because the complex interaction between living systems and nanoparticles are not fully understood. Such complexity derives from the ability of particles to bind and interact with biological matter while transforming their surface characteristics based on their external environment [11]. While TiO_2 NPs have been found to be absorbed at low levels in the GI tract, their exponential production and use in foods have raised concerns about potential toxicity due to chronic ingestion.[50] Nano-TiO_2, produced at a large scale for applications in many consumer products, have been classified as chemically and biologically inert without photoactivation.[51,52] Nano-TiO_2 becomes highly reactive under ultraviolet irradiation and produces reactive oxygen species (ROS) which can lead to strong antibacterial activity.[53,54] The mechanism of nanotoxicity for TiO_2 NPs has been suggested to be a production of ROS, which can alter proteins, RNA and DNA composition.[43] In contrast, some studies have reported few effects of TiO_2 NPs following exposure to mammalian systems and these conclusions could be due to different NPs dispersion states in those experiments.[54,55] Previous studies with the identical TiO_2 particles, concentrations, and exposure times showed that exposure of *L. rhamnosus* to TiO_2 NPs did not result in a loss of bacterial viability.[48] Additionally, experiments performed with TiO_2 of different sizes [100% rutile 17 nm, and rutile/anatase mixture M (37 & 9 nm) and P25 (48 & 55 nm)] demonstrated that, independently of their size, NPs were toxic and resulted in a decrease of *E. coli* viability at concentrations above 10 ppm.[44,54] This bacteria toxicity in response to TiO_2 NPs could be a result of the adsorption of NPs to the bacterial surface due to a gap of surface charge, highly oxidative radicals inducing ROS, a potential penetration of smallest NPs or abundance of aggregates in NPs suspensions.[44,54]

In the small intestine, secretion of gastrointestinal mucus by goblet cells (modeled in this study by HT29-MTX-E12) forms a gel that adheres at the mucosal surface to protect intestinal epithelial cells against shear forces that occur during the digestion process.[56] The GI mucus forms a single easily removable layer and a dense inner layer firmly attached to the epithelium not allowing bacteria to penetrate.[19,57] These mucus layers are organized around the highly glycosylated MUC2 mucin to form a net like structure that traps and transports debris and bacteria, lubricates, and lowers mechanical stress on the epithelium. By binding with bacteria and pathogenic viruses, mucus aids in digestion to immobilize enzymes near the epithelium surface, facilitating hydrolysis and absorption of nutrients.[30] Through this net like structure, several bacteria of the intestinal microbiota are able to penetrate and use the mucus glycans as a source of carbon and energy.[19] These properties emphasize the important role of mucus in human nutrition and health. Both the intestinal microbiota and the mucus play an important role in digestive health. Despite its classification as a major player in human nutrition and health, the microbiota have often been neglected in food toxicology in the context of nanoparticles, either separately or together[20]. Decades ago, data pertaining to the interaction between the mucus and TiO_2 NPs using *in vitro* co-culture model of Caco-2/HT29 was still in its infancy.[7,58] As of today, however, studies have been conducted to further understand this interaction. Through experimental studies, researchers have reported that the translocation and accumulation of TiO_2 in the mucus layer were facilitated by the different factors such as exposure time and particle concentration.[9,58] It has also been shown that TiO_2 NPs permeate the mucus layer and penetrate into the epithelial tissues in *ex vivo* studies performed on porcine buccal mucosa.[20] The findings in this study are significant because they shed light on the effects of acute exposure to TiO_2 NPs and the implications on overall intestinal health. These effects include thickness of the mucus layer, and changes in mucin composition (amounts of neutral and acidic mucins and proportions of sulfated and sialylated mucins). Possible toxicity-driven health conditions such as inflammatory bowel diseases, ulcerative colitis and Crohn's disease are generally linked to an alteration in mucosal integrity.[19] With studies showing the correlation between oral exposure to NPs and damages in the GI tract lining, it is important that physical and chemical properties of the GI tract are thoroughly assessed including the intestinal mucus layer.

Previously, *in vivo* studies performed on rats to determine the effects of induced ROS on colonic mucins showed that high levels of ROS significantly reduced the mucus barrier function by causing a decrease in mucus thickness by up to 50%.[59] With such reduction in the colonic mucus barrier, an increased levels of oxidant stress and decreased levels of antioxidant defense are witnessed, particularly in patients with active ulcerative colitis.[60,61] As MUC2 is the major secretory mucin synthesized and secreted by goblet cells, a wide array of bioactive factors, including cholinergic agonist, hormones (neuropeptides), microbes and microbial products and toxins, inflammatory cytokines, and reactive oxygen and nitrogen species have triggered massive secretion of MUC2 mucin by exocytosis in stimulated secretion.[14,62,63] Excessive increase in mucin production has also been observed in patients with cystic fibrosis, whereas production of abnormally glycosylated mucins have been found in patients with familial polyposis coli, ulcerative colitis, and colon cancer.[45] Similarly, previous work has shown that TiO_2 NPs induce ROS in an *in vitro* intestinal model, and it is possible that any decrease observed in the thickness of the mucus following exposure to TiO_2 NPs is due to ROS[8,48]. There are difficulties in the evaluation of the effects of NPs on the gut *in vivo* due to differences in species and variability in mucus composition. Additional studies focusing on physico-chemical properties of mucins and the microbiota will be needed to further look into and determine changes in mucus layer function caused by ROS.

Studies performed on germ-free rats have shown that positive influence on mucus thickness and composition was exerted by the presence of microflora throughout the GI tract.[64,65] Cellular damage to the biological systems has been reported to be caused by several nanoparticles as they accumulate within the system. These biological changes in the human system are mainly brought about by concentration,

electrical charges, particle-size distribution and interfacial characteristics.[13,66] Thus, toxicity assessments of NP ingestion and bacteria interactions are important since TiO_2 NPs have been classified as potentially carcinogenic for humans through inhalation.[43] In the current study, cells exposed to *L. rhamnosus* and *E. coli* showed an increased mucus thickness and changes in secretion of both neutral and acidic mucins. These results include increases in thickness of the mucus layer in the presence of bacteria or bacteria/TiO_2 NPs (**Figure 3B, C**). Exposure to *E. coli* led to an increase of the secretion of neutral mucins when alone or digested. These findings show that the presence of undigested TiO_2 NPs alone or with bacteria has an impact on the mucus layer function and can cause mucus secretion to be increased or decreased in the gut depending on exposure. Bacterial components recognized by mucus secreting cells also lead to an increase in secretion and production of mucins in order to fight against the presence of possible pathogens. Some invasive *E. coli* strains are known to be associated with Crohn's disease, mainly because they possess a protease that is involved in mucins degradation and therefore decrease mucus viscosity.[19] Nanosized TiO_2 has been reported to be toxic to *E. coli* in the presence of sunlight as it leads to the production of ROS.[53] TiO_2 NPs can induce ROS and DNA damage in *E. coli*, which can produce a protein that can induce mucus release and enhance bacterial colonization of the mucosa.[21,67] This protein belongs to a family of molecules that appear to modulate both adherence to epithelial cells and intestinal colonization. However, studies demonstrating whether TiO_2 NPs directly affect such proteins by inducing ROS or DNA damage are lacking.

A decrease in the thickness of the mucus layer could affect its integrity by making it permeable to pathogens and allowing the pathogens to penetrate and infiltrate the intestinal epithelium and lead to inflammation.[19,29] The rheological properties of mucus have been proven to be pH dependent, mucus it is a viscous solution at neutral pH and a gel in acidic conditions.[68] Since the mucus layer of the intestinal epithelial surface consists primarily of neutral mucins, an alteration in the function of the mucosa as a protective barrier can be indicative of a decrease in neutral mucins concentration. In the current study it was necessary to stain the cell co-cultures with the combined AB/PAS method to determine if there were changes in pattern or distribution of both mucin types which could be indicative of pathology.[14,63] Studies that have compared germ-free mice and conventionally raised animals demonstrated that microflora have significant effects on mucus composition and thickness. Furthermore, germ-free mice had a higher percentage of neutral and sulphated mucins with a relatively thinner mucus layer.[21] Additionally, certain intestinal microbes have been shown to induce mucin changes during infection in the GI tract by inducing the production of acidic mucins at the cost of neutral mucins, therefore changing its viscoelastic properties.[68] In this work, we found that the co-exposure to TiO_2 NPs and bacteria yields different results in each type of mucosubstances secretion as well as mucus thickness compared to individual exposure. Upon co-exposure to *L. rhamnosus* with pristine TiO_2 NPs, an increase in both neutral and acidic mucins was observed, which is indicative of barrier integrity enhancement to act as a trap to prevent NPs from reaching and penetrating the intestinal epithelial surfaces. On the contrary, co-exposure to *L. rhamnosus* and digested TiO_2 NPs led to no change of the neutral and acidic mucins secretions. The mucus thickness following exposure to *L. rhamnosus* and digested TiO_2 NPs was slightly increased when compared to controls but decreased when compared to L. rhamnosus only. This may be due to the fact that bacteria are able to induce mucin degradation by expressing specific proteins through enzymatic activities to attach to mucins glycoproteins.[19] Co-exposure to digested TiO_2 NPs and *E. coli* decreased neutral mucosubstances, possibly due to the secretion of proteins involved in mucin degradation and delivery of toxins to the cell surface, but increased mucus layer thickness when compared with all other conditions. The presence of microbiota in germ-free rats has been shown to influence thickness and composition of mucins. Particularly probiotic agents such as *Lactobacillus* species, can simulate mucin secretion in the intestine, improving pathogen resistance.[18,64] These findings validate results in this study and the increase in mucin secretion or mucus thickness observed in the presence of *L. rhamnosus*. Once impaired, the mucus barrier becomes susceptible to certain bacteria

species that are able to access the epithelial surface to cause inflammation, thus it is critical to maintain the integrity of the mucus layer through commensal residents.

4. Conclusion

In this work it was shown that exposure to TiO_2 NPs and commensal or opportunistic bacteria resulted in alterations to the thickness of the mucus layer in an *in vitro* GI tract model. It was found that there is an increase of mucus secretion in the presence of bacteria, which changes significantly upon co-exposure to NPs, suggesting that exposure to both commensal bacteria, opportunistic bacteria, and NP impacts the mucus layer. Independent exposure to physiologically relevant concentrations of digested TiO_2 NPs resulted in a decrease of the mucus thickness. When compared to negative controls, co-exposure to digested TiO_2 NPs and *E. coli* or *L. rhamnosus* resulted in a significant increase of mucus thickness. Higher amounts of acidic mucins were found in monolayers co-exposed to pristine TiO_2 NPs and bacteria, while co-exposure to digested TiO_2 NPs and bacteria showed no significant changes. An increase in neutral mucins was observed in the presence of both *E. coli* and *L. rhamnosus*, which was reversed when co-exposed with TiO_2 NPs. These results are significant as changes in the distribution or pattern of acidic and neutral mucins are indicative of certain pathological conditions. Overall, the *in vitro* model developed in this study provides a platform to enable the further understanding of the changes in the mucus layer, disease pathogenesis, and to develop novel therapeutic options such as the manipulation of the gut microbiota to address and diagnose chronic inflammatory gut diseases and show that interaction of ingested TiO_2 NPs with commensal bacteria and mucus layer can alter gut homeostasis.

5. Materials and Methods

All chemicals, enzymes and hormones were purchased from Sigma-Aldrich (St Louis, MO, USA) unless otherwise indicated. All culture plates, flasks, tubes and pipette tips used for cell culture were purchased from Corning Life Sciences. Glassware used in sample preparation and analysis was washed, soaked in 10% hydrochloric acid and rinsed with 18 MΩ de-ionized (DI) water. All other reagents were prepared in (18 mΩ) water or 1X phosphate-buffer saline in water.

5.1 Nanoparticle dose and preparation

This study is designed to expose an *in vitro* model of the GI tract to nanoparticles commonly used as food additives at physiologically relevant doses. The titanium dioxide (TiO_2) nanoparticles (30 nm, anatase, US3498US, Research Nanomaterials, Inc, Houston, TX) doses and characterization were previously described in detail.[8] **Table 1** shows physico-chemical properties of primary particles and behavior in dispersants. Once dispersed, TiO_2 NPs were serially diluted in DMEM supplemented with 10% (v/v) heat-inactivated fetal bovine serum (HI FBS, ThermoFisher Scientific, Waltham, MA, USA) or subjected to an *in vitro* digestion prior to measurements of *in vitro* exposures. A dose of 0.14 µg/mL was used for all *in vitro* experiments and all exposure times were 4 hours. The acute exposure of 4 hours is related to digestion time. It is the time it takes for the contents of the small intestine to transit.[8] This selected exposure time did not affect the viability of the cells, as barrier function is necessary to complete functional studies and is a better representation of particle settling following short-term digestion. The diameter of 30 nm, anatase TiO_2 is a model of TiO_2 NPs used as food additive. The exposure time and NPs diameter were equivalent to the ones used in previous studies.[8]

5.2 Nanoparticles Characterization

NP agglomerates were broken down by 30 min sonication (VWR® symphony™ Ultrasonic Cleaners, RF-48 W, 35k Hz operation frequency), and then diluted to final doses (**shown in Table 1**). TiO_2 NPs were sonicated in (18 MΩ) DI water and dispersed at 28mg/mL in 5 mL of solute in 20 mL, 28mm diameter borosilicate glass scintillation vials, by indirect sonication with an Ultrasonic Cleaner (VWR® symphony™ Ultrasonic Cleaners, RF-48 W, 35k Hz operation frequency, Radnor, PA). The sample container with the suspension was placed in the sonication bath for 30 min on continuous mode operation

with temperature starting at 21°C. The system was calibrated by the calorimetric calibration method described by Taurozzi, whereby the power delivered to the sample was determined to be 0.128 W.[8,69] The delivered sonication energy was measured from the calibrated delivered power over the continuous 30 min time period and determined to be 230 J. After sonication and dilution, the NP dispersants were used for determining NPs properties or exposure to the *in vitro* model. The properties of NPs, including distributions of digested NPs sizes, average ζ- potential, and Polydispersity index (PdI), were measured with Dynamic Light Scattering (DLS) using a Zetasizer Nano ZS (Malvern Instruments Inc, Southborough, MA), with Malvern disposable polycarbonate folded capillary cells (DTS1070).

5.3 Cell culture

A coculture of human colon carcinoma Caco-2, and mucus producing HT29-MTX-E12 cell lines were used to mimic the human small intestinal epithelial layer. The Caco-2 cell line was obtained from the American Type Culture Collection (Manassas, VA, USA) at passage 20 and experiments were conducted at passage 30-40. The human colon adenocarcinoma mucus-secreting cell line HT29-MTX-E12 was purchased from Sigma-Aldrich (Saint Louis, MO, USA) at passage 57 and was used in experiments at passage 65-75. Both cell lines were grown in Dulbecco's Modified Eagle Medium and (4.5 g/L) glucose, L-Glutamine (DMEM, Gibco®) supplemented with 10% (v/v) heat-inactivated fetal bovine serum (HI FBS, ThermoFisher Scientific, Waltham, MA, USA). Cells were maintained at 37 °C under 5% CO_2 and culture medium was changed every other day. For all experimental studies, cells were stained with trypan blue, counted using a hemocytometer, resuspended at a ratio of 3:1 Caco-2 to HT29-MTX. Cells were seeded at a density of (100,000 cells/cm^2) onto polycarbonate, (0.4 μm) pore size, (1.12 cm^2) Transwell® inserts, or at a density of (50,000 cells/cm^2) onto 24 well plates or (22X22 mm) glass coverslips within six well plates (Corning Life Sciences, Kennebunk, ME, USA) coated with rat tail Type I collagen (BD Biosciences, San Jose, CA) at 8 μg/cm^2. Previous work has shown that Caco-2/HT29-MTX monolayers seeded at 3:1 and grown for two weeks developed a (2-10 μm) thick mucus layer that covers the cell monolayer completely.[70] All experiments were performed on fully differentiated cells 14 days post-seeding.

5.4. Bacterial cultures

Caco-2/HT29-MTX and bacteria triculture methods have been described previously.[48] *Lactobacillus rhamnosus GG:pMF440* and *Escherichia coli ATCC 11775,* and *E. coli 10798:pMF440* were inoculated and grown in brain heart infusion media (BHI, Becton, Dickinson, Sparks, MD) in glass tubes for 48 and 24 hrs respectively. pMF440 is a broad host range plasmid containing the mCherry gene. Both microorganisms were kept at 37 °C and 5% CO_2. *L. rhamnosus* was grown in a static environment and *E. coli* in agitation (~150 rpm). Prior to inoculation, the concentration of bacteria was estimated by determining the optical culture density and using a calibration curve. Culture was then serially diluted, in DMEM, to a concentration of (10^3 CFU/mL) (approximately 263 CFU/cm^2). Previous work has shown that bacterial viability is unaffected following a 4 hr exposure to (0.14 μg/mL) TiO_2 NP.[75]

5.5. *In vitro* digestion/acute exposure

For the *in vitro* simulated digestions experiments, a detailed 3-phase (mouth, stomach, small intestine) gastrointestinal tract (GIT) simulator adapted from previous studies was used.[71] Briefly, TiO_2 nanoparticles were dispersed in (18 MΩ) sterile water in a scintillation vial (VWR™ International, LLC) and sonicated for 30 min using a bath sonicator (VWR® symphony™ Ultrasonic Cleaners, RF-48 W, 35k Hz operation frequency). In the mouth phase, a simulated mixture of salts solution (0.1 mL of 1M KCl, 0.3 mL of 1M $CaCl_2$ and 1.4 mL of NaCl) was added for 1-5 min. To initiate gastric digestion the pH was adjusted to pH 2.0 with (1M) HCl, (1 mL) of pepsin solution (0.1 g in 0.1M HCl) was added, and the solution was rocked on a rocker for 1 hour at 55 oscillations/min at 37 °C to mimic the digestion phase in the stomach. Following gastric incubation, the pH of the sample (also referred to as the "digest") was raised to 5.5- 6 with (1M) $NaHCO_3$ and mixed with (5.25 mL) of simulated intestinal fluid with bile salts/porcine pancreatin (0.05 g of porcine pancreatin and (0.3 g) of porcine bile extract in (0.1 M)

$NaHCO_3$ for 2 hours. The pH was then adjusted to 6.9-7.0 with 1M $NaHCO_3$ and the final volume was increased to (20 mL) with (140 mM) NaCl, (5 mM) KCl. The samples were then considered digests or digested NP to help differentiate from pristine (non-digested) TiO_2.

For acute (4hr) exposure, cells were grown to confluency and allowed to differentiate for 14 days post-seeding while changing the culture medium at least 3 times per week. Fully differentiated cells were exposed to a total volume of (0.5 mL) (for 24 well plates and 12 well plate Transwells) or (2 mL) (for 6 well plates) of prepared digested TiO_2 or TiO_2-free and bacteria-free digest, bacteria and/or pristine TiO_2 diluted in DMEM for 4 hours. To recreate these physiologically relevant doses on a surface area basis *in vitro*, the amount of ingested NP was divided by the surface area of the human small intestine (2×10^6 cm^2), which is described as the medium or average dose. High doses were two orders of magnitude higher than medium dose (**Table 1**). The properties of digested NP, including distributions of digested NP sizes, average ζ- potential, and Polydispersity index (PdI), were measured with Dynamic Light Scattering (DLS) using a Zetasizer Nano ZS (Malvern Instruments Inc, Southborough, MA), with Malvern disposable polycarbonate folded capillary cells (DTS1070).[8] *In vitro* dosage used was estimated and rationalized according to the estimated daily human intake of NPs and the surface area of human small intestinal epithelium. TiO_2 NP intake has previously been estimated to be 0.2-0.7 mg/kg body weight/day for Western adults and 36% of the NPs is in the nanoscale, meaning that approximately 25 mg of nano-TiO_2 is consumed daily.[5] Doses in this study were deemed relevent to reflect real-life exposure from a single meal and equivalent to the high dose used in previous work.[8] The acute dosage seems to be a more accurate exposure estimate as ingested materials move through GI tract. The limitation of added TiO_2 NPs is set to 1% of the overall food weight in the United States.[72]

5.6. Mucus layer characterization

A modification of well-established Alcian Blue methods were used to visualize and quantify the mucus layer coverage, and quantify the acidic mucosubstances.[56,73,74] Co-cultures of Caco-2/HT29-MTX were performed on well plates rather than inserts for these assays. Following acute exposure to NP and/or bacteria, the cells were carefully washed with PBS and fixed with 4% paraformaldehyde in 1X PBS, pH 4.0 for 30 minutes at room temperature. The fixing solution was then replaced with alcian blue (pH 2.5) dissolved in acetic acid to visualize acidic mucosubstances attached to the cells. Following incubation at RT for 30-40 min in the dark, cells were rinsed until supernatant was clear and images were captured using brightfield microscope (brand name). After images were taken, the intensity of the alcian blue was also quantified by lysing the stained cells with acetic acid and depositing the supernatant following centrifugation in 96-well plates. Absorbance was measured at (630 nm) with a plate reader (Gen5™, BioTek Synergy Instruments Inc, Vermont, USA). A Periodic Acid-Schiff (PAS) assay was also performed to quantify secretion of neutral mucins and sialic acid containing mucosubstances. Following exposure to bacteria and nanoparticles, cells were lysed with 10% Triton-X 100 in 1X PBS and triplicate of aliquots (30 μL) of each cell lysate were then transferred onto 96-well plates where (120 μL) of 0.6% periodic acid was added to the lysate containing wells and incubated at RT for 90 minutes under little agitation; followed by (100 μL) of Schiff reagent for 40 minutes in the dark without agitation. Plates were then read at 550 nm to measure absorbance using a plate reader. Standard curves for both assays were prepared using stomach porcine mucin with increasing concentrations (0-3500 μg/mL).

5.7. Histology of mucus secreted by HT29-MTX-E12 cells

Cocultures of Caco-2 and HT29-MTX-E12 were seeded onto polycarbonate, (0.4 μm) pore size, (12-mm) Transwell inserts (VWR, Radnor, PA, USA) at a density of 100,000 cells/cm^2 for histochemical evaluation. After 14 days post-seeding, culture medium was removed and cells were exposed to physiologically relevant doses of TiO_2 and bacteria for 4 hr; fixed with 4% paraformaldehyde in 1X PBS, pH 4.0 for 30 min at room temperature and rinsed with PBS. HistoGel (Thermo Scientific, Richard-Allen Scientific, Kalamazoo, MI, USA) was liquified by heating to 60°C and roughly 0.5 mL was added to the

apical side of the polycarbonate membrane. Once HistoGel had cooled and solidified, the membranes were removed with a disposable scalpel (Electron Microscopy Sciences, Hatfield, PA) and embedded in paraffin. Thin sections were transversely cut and stained with combined alcian blue (pH 2.5; 8GX, Alfa Aesar, Wardwill, MA) and PAS to visualize the mucus layer thickness and acidic, neutral and sialic acid containing mucosubstances attached to the monolayer.

5.8. Confocal laser scanning microscopy of bacteria and TiO_2 interaction with mucus layer from coculture (Caco-2/HT29-MTX-E12)

Secretion of mucus by the coculture and its interaction with bacteria distribution was observed at a concentration of 10^3 CFU/mL using laser confocal microscopy (LSM 880, Carl Zeiss Microscopy, LLC) equipped with an oil immersion objective (PL APO 63x/1.40 oil DIC, Carl Zeiss Microscopy, LLC). *In vitro* co-cultures were seeded onto sterile microscope glass coverslips coated with 8 μg/cm^2 of collagen Type I in 6 well plates at a density of 50,000 cells/cm^2. After 2 weeks of culture and exposure to TiO_2 and/or bacteria, cells were fixed with 4% paraformaldehyde (PFA) for 30 minutes at room temperature and rinsed with PBS. The cell membrane, nucleus and mucus layer were stained using fluorochromes Cellmask™ Deep Red plasma membrane stain (C10046, Life Technologies, USA), Hoechst 33342, and wheat germ agglutinin (WGA, Alexa Fluor® 488 conjugate, Invitrogen) diluted in 1X PBS for 15 min in the dark at concentrations of 1/1000, 1/500 and 1/200 respectively. Samples were then rinsed, air-dried and coverslips were removed from 6 well plates to be mounted on a glass slide with ProLong® Gold (Thermofisher Scientific, USA) and dried overnight in the dark. Z stack images were taken the following day and images were processed using Zen and ImageJ software (Cornell, Ithaca, USA).

5.9. Statistical Analysis

Results are expressed as mean ± standard error. Analyses of mucosubstances composition in the *in vitro* model were performed using the software package GraphPad Prism version 5.0 for Windows (GraphPad Software, San Diego, California, USA). Kolmogorov-Smirnov and D'Agostino and Pearson omnibus normality test were performed prior to one-way ANOVA (Analysis of Variance) with Tukey's post-test to assess for statistical differences between the various means of each series of experiments. Differences between means were considered statistically not significant when the P-value was > 0.05. Mucus thickness was measured (50 measurements per section / 3-6 sections per sample / 3 samples per condition) using IBM SPSS Statistics version 25's one-way ANOVA post hoc test Duncan with $P < 0.05$.

6. Conflict of Interest Statement

The authors declare that the research was conducted in the absence of any relationships that could be construed as a potential conflict of interest.

7. Acknowledgements

This work was supported by the National Institutes of Health grant no. 1R01ES028788. This material is based upon work also supported by the Louis Stokes Alliance for Minorities Program Bridge to Doctorate (LSAMP BD) fellowship and Gates Millennium Scholarship. Jacob V. Tanzman and Kyle F. Cullin are thanked for providing the mCherry bacterial strains. Melissa Mendoza, Chukwuazam A. Nwasike and Ian M. Claydon are thanked for their assistance with assays and calculations. Any findings, conclusions or recommendations expressed in this material are those of the author(s) and do not necessarily reflect the views of the National Institutes of Health. All authors read and approved the final submission of the manuscript.

References:

[1] M. Rai, A. Yadav, A. Gade, *Biotechnol. Adv.* 2009, *27*, 76.

[2] D. E. Lefebvre, K. Venema, L. Gombau, L. G. V. Jr, J. Raju, G. S. Bondy, H. Bouwmeester, R. P. Singh, A. J. Clippinger, E.-M. Collnot, R. Mehta, V. Stone, *Nanotoxicology* 2015, *9*, 523.

[3] H. Bouwmeester, S. Dekkers, M. Y. Noordam, W. I. Hagens, A. S. Bulder, C. de Heer, S. E. C. G. ten Voorde, S. W. P. Wijnhoven, H. J. P. Marvin, A. J. A. M. Sips, *Regul. Toxicol. Pharmacol.* 2009, *53*, 52.

[4] B. Viswanath, S. Kim, in *Rev. Environ. Contam. Toxicol. Vol. 242*, Springer, Cham, 2016, pp. 61–104.

[5] A. Weir, P. Westerhoff, L. Fabricius, K. Hristovski, N. von Goetz, *Environ. Sci. Technol.* 2012, *46*, 2242.

[6] J. J. Faust, K. Doudrick, Y. Yang, P. Westerhoff, D. G. Capco, *Cell Biol. Toxicol.* 2014, *30*, 169.

[7] E. Brun, F. Barreau, G. Veronesi, B. Fayard, S. Sorieul, C. Chanéac, C. Carapito, T. Rabilloud, A. Mabondzo, N. Herlin-Boime, M. Carrière, *Part. Fibre Toxicol.* 2014, *11*, 13.

[8] Z. Guo, N. J. Martucci, F. Moreno-Olivas, E. Tako, G. J. Mahler, *NanoImpact* 2017, *5*, 70.

[9] M. Dorier, D. Béal, C. Marie-Desvergne, M. Dubosson, F. Barreau, E. Houdeau, N. Herlin-Boime, M. Carriere, *Nanotoxicology* 2017, *11*, 751.

[10] R. J. B. Peters, G. van Bemmel, Z. Herrera-Rivera, H. P. F. G. Helsper, H. J. P. Marvin, S. Weigel, P. C. Tromp, A. G. Oomen, A. G. Rietveld, H. Bouwmeester, *J. Agric. Food Chem.* 2014, *62*, 6285.

[11] A. Elsaesser, C. V. Howard, *Adv. Drug Deliv. Rev.* 2012, *64*, 129.

[12] N. Sozer, J. L. Kokini, *Trends Biotechnol.* 2009, *27*, 82.

[13] N. Pradhan, S. Singh, N. Ojha, A. Shrivastava, A. Barla, V. Rai, S. Bose, "Facets of Nanotechnology as Seen in Food Processing, Packaging, and Preservation Industry," DOI 10.1155/2015/365672can be found under https://www.hindawi.com/journals/bmri/2015/365672/, 2015.

[14] Y. S. Kim, S. B. Ho, *Curr. Gastroenterol. Rep.* 2010, *12*, 319.

[15] S. Bellmann, D. Carlander, A. Fasano, D. Momcilovic, J. A. Scimeca, W. J. Waldman, L. Gombau, L. Tsytsikova, R. Canady, D. I. A. Pereira, D. E. Lefebvre, *Wiley Interdiscip. Rev. Nanomed. Nanobiotechnol.* 2015, *7*, 609.

[16] I. L. Bergin, F. A. Witzmann, *Int. J. Biomed. Nanosci. Nanotechnol.* 2013, *3*, 163.

[17] P. Dharmani, V. Srivastava, V. Kissoon-Singh, K. Chadee, *J. Innate Immun.* 2009, *1*, 123.

[18] D. R. Mack, S. Michail, S. Wei, L. McDougall, M. A. Hollingsworth, *Am. J. Physiol.-Gastrointest. Liver Physiol.* 1999, *276*, G941.

[19] J.-F. Sicard, G. Le Bihan, P. Vogeleer, M. Jacques, J. Harel, *Front. Cell. Infect. Microbiol.* 2017, *7*, DOI 10.3389/fcimb.2017.00387.

[20] M. Mercier-Bonin, B. Despax, P. Raynaud, E. Houdeau, M. Thomas, *Crit. Rev. Food Sci. Nutr.* 2018, *58*, 1023.

[21] S. Cornick, A. Tawiah, K. Chadee, *Tissue Barriers* 2015, *3*, DOI 10.4161/21688370.2014.982426.

[22] L. C. Prasanna, *J. Clin. Diagn. Res. JCDR* 2016, *10*, AC01.

[23] R. Nonose, A. P. P. Spadari, D. G. Priolli, F. R. Máximo, J. A. Pereira, C. A. R. Martinez, *Acta Cir. Bras.* 2009, *24*, 267.

[24] S. S. SPICER, T. J. LEPPI, P. J. STOWARD, *J. Histochem. Cytochem.* 1965, *13*, 599.

[25] M. E. V. Johansson, H. E. Jakobsson, J. Holmén-Larsson, A. Schütte, A. Ermund, A. M. Rodríguez-Piñeiro, L. Arike, C. Wising, F. Svensson, F. Bäckhed, G. C. Hansson, *Cell Host Microbe* 2015, *18*, 582.

[26] H. Sinnecker, T. Krause, S. Koelling, I. Lautenschläger, A. Frey, *Beilstein J. Nanotechnol.* 2014, *5*, 2092.

[27] S. Jalili-Firoozinezhad, F. S. Gazzaniga, E. L. Calamari, D. M. Camacho, C. W. Fadel, A. Bein, B. Swenor, B. Nestor, M. J. Cronce, A. Tovaglieri, O. Levy, K. E. Gregory, D. T. Breault, J. M. S. Cabral, D. L. Kasper, R. Novak, D. E. Ingber, *Nat. Biomed. Eng.* 2019, *3*, 520.

[28] C. Atuma, V. Strugala, A. Allen, L. Holm, *Am. J. Physiol.-Gastrointest. Liver Physiol.* 2001, *280*, G922.
[29] M. E. V. Johansson, H. E. Jakobsson, J. Holmén-Larsson, A. Schütte, A. Ermund, A. M. Rodríguez-Piñeiro, L. Arike, C. Wising, F. Svensson, F. Bäckhed, G. C. Hansson, *Cell Host Microbe* 2015, *18*, 582.
[30] L. Montagne, C. Piel, J. P. Lalles, *Nutr. Rev.* 2004, *62*, 105.
[31] A. Walczak, E. Kramer, P. Hendriksen, P. Tromp, J. Helsper, M. van der Zande, I. Rietjens, H. Bouwmeester, *Nanotoxicology* 2014, *9*, 1.
[32] W. M. Saltzman, M. L. Radomsky, K. J. Whaley, R. A. Cone, *Biophys. J.* 1994, *66*, 508.
[33] S. K. Lai, Y.-Y. Wang, J. Hanes, *Adv. Drug Deliv. Rev.* 2009, *61*, 158.
[34] M. Zhang, K. Sun, Y. Wu, Y. Yang, P. Tso, Z. Wu, *Front. Immunol.* 2017, *8*, DOI 10.3389/fimmu.2017.00942.
[35] M. Elderman, B. Sovran, F. Hugenholtz, K. Graversen, M. Huijskes, E. Houtsma, C. Belzer, M. Boekschoten, P. de Vos, J. Dekker, J. Wells, M. Faas, *PLoS ONE* 2017, *12*, DOI 10.1371/journal.pone.0184274.
[36] J. Gerritsen, H. Smidt, G. T. Rijkers, W. M. de Vos, *Genes Nutr.* 2011, *6*, 209.
[37] P. C Konturek, T. Brzozowski, S. J. Konturek, *Stress and the Gut: Pathophysiology, Clinical Consequences, Diagnostic Approach and Treatment Options*, 2011.
[38] R. M. McLoughlin, K. H. G. Mills, *J. Allergy Clin. Immunol.* 2011, *127*, 1097.
[39] L.-Y. Liu, L. Sun, Z.-T. Zhong, J. Zhu, H.-Y. Song, *Nucl. Sci. Tech.* 2016, *27*, 5.
[40] R. Khan, F. C. Petersen, S. Shekhar, *Front. Immunol.* 2019, *10*, DOI 10.3389/fimmu.2019.01203.
[41] K. Qiu, P. G. Durham, A. C. Anselmo, *Nano Res.* 2018, *11*, 4936.
[42] G. Pinget, J. Tan, B. Janac, N. O. Kaakoush, A. S. Angelatos, J. O'Sullivan, Y. C. Koay, F. Sierro, J. Davis, S. K. Divakarla, D. Khanal, R. J. Moore, D. Stanley, W. Chrzanowski, L. Macia, *Front. Nutr.* 2019, *6*, DOI 10.3389/fnut.2019.00057.
[43] W. Dudefoi, K. Moniz, E. Allen-Vercoe, M.-H. Ropers, V. K. Walker, *Food Chem. Toxicol.* 2017, *106*, 242.
[44] J. Nesic, S. Rtimi, D. Laub, G. M. Roglic, C. Pulgarin, J. Kiwi, *Colloids Surf. B Biointerfaces* 2014, *123*, 593.
[45] J. R. Gum, J. C. Byrd, J. W. Hicks, N. W. Toribara, D. T. Lamport, Y. S. Kim, *J. Biol. Chem.* 1989, *264*, 6480.
[46] D. W. Kufe, *Nat. Rev. Cancer* 2009, *9*, 874.
[47] J. M. Holmén Larsson, K. A. Thomsson, A. M. Rodríguez-Piñeiro, H. Karlsson, G. C. Hansson, *Am. J. Physiol. - Gastrointest. Liver Physiol.* 2013, *305*, G357.
[48] J. W. Richter, G. M. Shull, J. H. Fountain, Z. Guo, L. P. Musselman, A. C. Fiumera, G. J. Mahler, *Nanotoxicology* 2018, *12*, 390.
[49] D. Hanaor, M. Michelazzi, C. Leonelli, C. C. Sorrell, *J. Eur. Ceram. Soc.* 2012, *32*, 235.
[50] J. Li, S. Yang, R. Lei, W. Gu, Y. Qin, S. Ma, K. Chen, Y. Chang, X. Bai, S. Xia, C. Wu, G. Xing, *Nanoscale* 2018, *10*, 7736.
[51] B. K. Bernard, M. R. Osheroff, A. Hofmann, J. H. Mennear, *J. Toxicol. Environ. Health* 1990, *29*, 417.
[52] R. C. Lindenschmidt, K. E. Driscoll, M. A. Perkins, J. M. Higgins, J. K. Maurer, K. A. Belfiore, *Toxicol. Appl. Pharmacol.* 1990, *102*, 268.
[53] Chang. Wei, W. Yuan. Lin, Zulkarnain. Zainal, N. E. Williams, Kai. Zhu, A. P. Kruzic, R. L. Smith, Krishnan. Rajeshwar, *Environ. Sci. Technol.* 1994, *28*, 934.
[54] M. Planchon, R. Ferrari, F. Guyot, A. Gélabert, N. Menguy, C. Chanéac, A. Thill, M. F. Benedetti, O. Spalla, *Colloids Surf. B Biointerfaces* 2013, *102*, 158.
[55] B. Rehn, F. Seiler, S. Rehn, J. Bruch, M. Maier, *Toxicol. Appl. Pharmacol.* 2003, *189*, 84.
[56] S. Kerss, A. Allen, A. Garner, *Clin. Sci.* 1982, *63*, 187.

[57] J. B. J. Kamphuis, M. Mercier-Bonin, H. Eutamène, V. Theodorou, *Sci. Rep.* 2017, *7*, 8527.
[58] K. Gillois, M. Lévêque, V. Théodorou, H. Robert, M. Mercier-Bonin, *Microorganisms* 2018, *6*, 53.
[59] I. A. Brownlee, J. Knight, P. W. Dettmar, J. P. Pearson, *Free Radic. Biol. Med.* 2007, *43*, 800.
[60] R. D. Pullan, G. A. Thomas, M. Rhodes, R. G. Newcombe, G. T. Williams, A. Allen, J. Rhodes, *Gut* 1994, *35*, 353.
[61] V. Strugala, P. W. Dettmar, J. P. Pearson, *Int. J. Clin. Pract.* 2008, *62*, 762.
[62] C. W. Davis, B. F. Dickey, *Annu. Rev. Physiol.* 2008, *70*, 487.
[63] A. A. Weiss, M. W. Babyatsky, S. Ogata, A. Chen, S. H. Itzkowitz, *J. Histochem. Cytochem.* 1996, *44*, 1161.
[64] L. Szentkuti, H. Riedesel, M.-L. Enss, K. Gaertner, W. von Engelhardt, *Histochem. J.* 1990, *22*, 491.
[65] L. Szentkuti, M.-L. Enss, *Comp. Biochem. Physiol. A. Mol. Integr. Physiol.* 1998, *119*, 379.
[66] B. Chen, J. R. G. Evans, *Carbohydr. Polym.* 2005, *61*, 455.
[67] P. Kumar, Q. Luo, T. J. Vickers, A. Sheikh, W. G. Lewis, J. M. Fleckenstein, *Infect. Immun.* 2014, *82*, 500.
[68] J. P. Celli, B. S. Turner, N. H. Afdhal, R. H. Ewoldt, G. H. McKinley, R. Bansil, S. Erramilli, *Biomacromolecules* 2007, *8*, 1580.
[69] J. S. Taurozzi, V. A. Hackley, M. R. Wiesner, *Preparation of Nanoparticle Dispersions from Powdered Material Using Ultrasonic Disruption - Version 1.1*, National Institute Of Standards And Technology, 2012.
[70] G. J. Mahler, M. B. Esch, R. P. Glahn, M. L. Shuler, *Biotechnol. Bioeng.* 2009, *104*, 193.
[71] R. P. Glahn, O. A. Lee, A. Yeung, M. I. Goldman, D. D. Miller, *J. Nutr.* 1998, *128*, 1555.
[72] "CFR - Code of Federal Regulations Title 21," can be found under https://www.accessdata.fda.gov/scripts/cdrh/cfdocs/cfcfr/cfrsearch.cfm?fr=73.575, n.d.
[73] B. Sandzén, H. Blom, S. Dahlgren, *Scand. J. Gastroenterol.* 1988, *23*, 1160.
[74] A. Wikman, J. Karlsson, I. Carlstedt, P. Artursson, *Pharm. Res.* 1993, *10*, 843.
[75] A. Garcia-Rodriguez, F. Moreno-Olivas, R. Marcos, E. Tako, C. N. H. Marques, G. J. Mahler. *Pending J. 2019*, Submitted.

Figures Legends

Table 1. Characterization of digested and undigested TiO_2 NPs in DMEM and in simulated gastrointestinal tract fluid. Hydrodynamic size ($d_{h,z\text{-average}}$), polydispersity index (PdI), and zeta potential (ζ) of 30 nm TiO_2 NPs concentrations were measured. Data are shown as mean ± SEM. ($p<0.05$), $n \geq 3$ independent measurements.

Figure 1. Acidic mucins stained with Alcian blue and imaged (20x magnification) (**A**) Caco-2 monolayer, (**B**) HT29-MTX-E12 monolayer and (**C**) Caco-e/HT29-MTX-E12 monolayer or quantified based on alcian blue color intensity in *in vitro* model (Caco-2/HT29-MTX-E12) following individual exposure to undigested TiO_2 NPs, bacteria or co-exposure to either *E. coli* or *L. rhamnosus* (**D, F**) and digested TiO_2 NPs co-exposed to either bacteria respectively (**E, G**). Results are expressed relative to each column as mean standard error, and considered significantly different with *$p<0.05$, $n=12$ using a one-way ANOVA (Analysis of Variance) with Tukey's post-test. Bars that do not share any letters are significantly different. CT – DMEM only, DG – digest.

Figure 2. Quantification of neutral mucins based on periodic acid-Schiff staining method following exposure to TiO_2 NPs and/or bacteria. Undigested (**A, C**) and digested (**B, D**) conditions showing different alterations in mucus secretion. A one-way ANOVA (Analysis of Variance) with Tukey's post-

test was used to determine statistical differences between the different means with p values < 0.05. Bars that do not share any letters are significantly different.

Figure 3. Cross-sectional images of HT29-MTX-E12 cell monolayer (**A**) stained with AB/PAS showing both acidic and neutral mucins with an average mucus thickness 8.8976 ± 0.241 μm. Blue color represents Acidic mucins (AC), Magenta color – Neutral mucins (NC) and deep dark purple – both mucins types and sialic acid containing mucosubstances together. **B** and **C** represent quantification of mucus thickness following co-exposure to digested TiO_2 NPs with *E. coli* or *L. rhamnosus*.

Table 2. Representation of average mucus thickness following exposure to digested TiO_2 NPs and/or bacteria. Results represented as mean ± standard error mean (SEM). Bars that do not share letters are significantly different according to one-way ANOVA with Tukey's posttest $p < 0.05$.

Figure 4. Confocal images (orthogonal views) of Caco-2/HT29-MTX-E12 *in vitro* barrier. Z-scans were performed where monolayer was stained with appropriate fluorochromes. Confocal microscope was used to differentiate the components of *in vitro* model, **(A)** control, **(D)** digested NPs, **(E)** digested NPs and *E. coli*, and **(F)** digested NPs and *L. rhamnosus*. Mucus in green, and cell nucleus in blue, both *E. coli* and *L. rhamnosus* in expressed in red (**B, C, E, F**), and NPs reflection in white over the mucus layer **(D)** (scale bar = 20 μm).

Figure 5. Transversal cuts of Caco-2/HT29-MTX-E12 *in vitro* barrier. Further analysis of the Z-scans was performed to study the interaction between TiO_2 and/bacteria with the mucus layer following a 4hr exposure. **A**) barrier and DMEM only **B**) barrier and digested TiO_2 NPs, **C**) barrier, *E. coli* **D**) digested TiO_2 NPs and *E. coli* **E**) barrier, *L. rhamnosus* **F**) digested TiO_2 NPs and *L. rhamnosus*. Mucus is stained in green, cell nucleus in blue and bacteria in red. (scale bar = 20 μm). NP was not reflective enough to be seen due to the intensity of mucus stain. White circles indicate bacteria entrapped in the mucus layer.